3rd WORKSHOP ON PARTICLE PHYSICS

NATIONAL CENTRE FOR PHYSICS
(QUAID-I-AZAM UNIVERSITY)

Detectors for High Energy Physics

Lecture III - Tracking

Gigi Rolandi – Cern – Geneva - Switzerland

http://rolandi.home.cern.ch/rolandi/

edit: F. Bedeschi, M. Diemoz, F. Gianotti, C. Joram, J. Virdee

Detection of particles

Particles are detected through their interaction with the detector

In the following we will study in a quantitative way the interaction of charged and neutral particles with matter

harged particle through matter

- Scatter on nuclei (m << $M_{nucleus}$) without loosing energy
- Loose energy interacting with atomic electrons (m_e << m) without changing direction

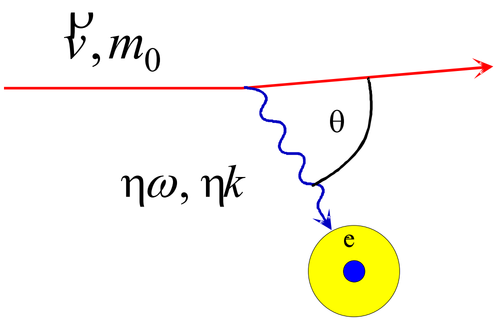

$$\left\langle \frac{dE}{dx} \right\rangle = -\int_0^\infty N E \frac{d\sigma}{dE} \eta \, d\omega$$

N : electron density

If hω is large enough the atom is ionized

stead of ionizing an atom, under certain conditions the photon can so escape from the medium.

› Emission of **Cherenkov** and **Transition radiation.**

Scattering

An incoming particle with charge z interacts with
target of nuclear charge Z. The cross-section
r this e.m. process is

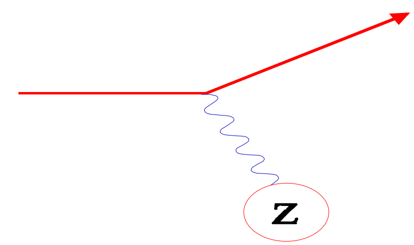

Rutherford formula

$$\frac{d\sigma}{d\Omega} = 4 zZr_e^2 \left(\frac{m_e c}{\beta p} \right)^2 \frac{1}{\sin^4 \theta/2} \qquad \langle \theta \rangle = 0$$

verage scattering angle
ross-section for $\theta \to 0$ infinite !

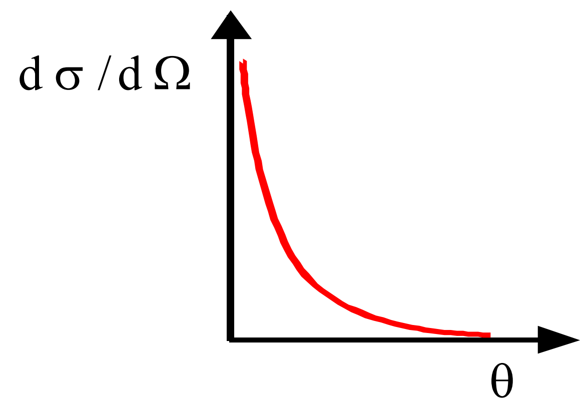

Multiple Scattering

ufficiently thick material layer → the particle will undergo multiple cattering.

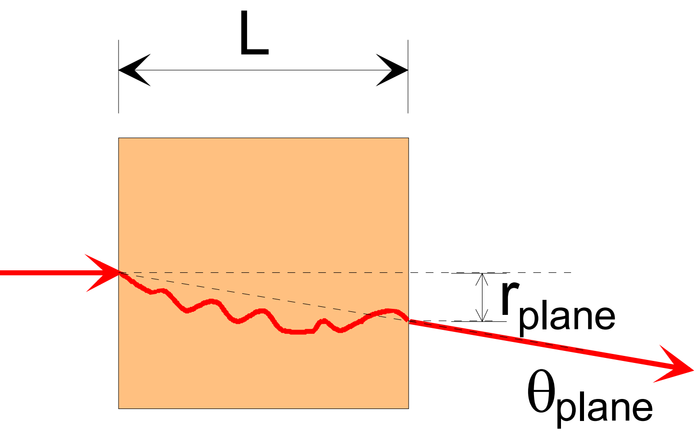

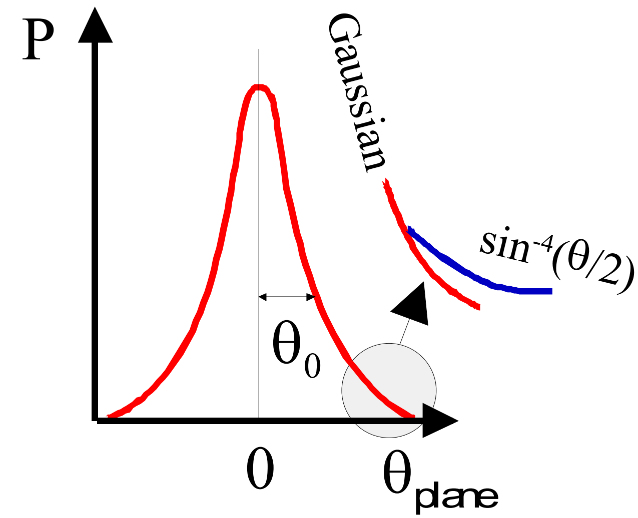

$$\theta_0 = \theta_{plane}^{RMS} = \sqrt{\left\langle \theta_{plane}{}^2 \right\rangle} = \frac{1}{\sqrt{2}} \theta_{space}^{RMS}$$

Approximation :

$$\theta_0 \propto \frac{1}{p}\sqrt{\frac{L}{X_0}}$$

X_0 is radiation length of the medium

Multiple scattering contribution to momentum error

$$\frac{\sigma(p)}{p_T} \propto \sigma(x) \cdot p_T \quad \text{and} \quad \sigma(x)\Big|^{MS} \propto \theta_0 \propto \frac{1}{p} \quad \Longrightarrow \quad \frac{\sigma(p)}{p_T}\Bigg|^{MS} = \text{constant}$$

independent of p !

More precisely:

$$\frac{\sigma(p)}{p_T}\Bigg|^{MS} = \frac{0.045}{B(T)\sqrt{L(m)X_0(m)}}$$

ex: Ar (X_0=110m), L=1m, B=1T

$$\frac{\sigma(p)}{p_T}\Bigg|^{MS} \approx 0.5\%$$

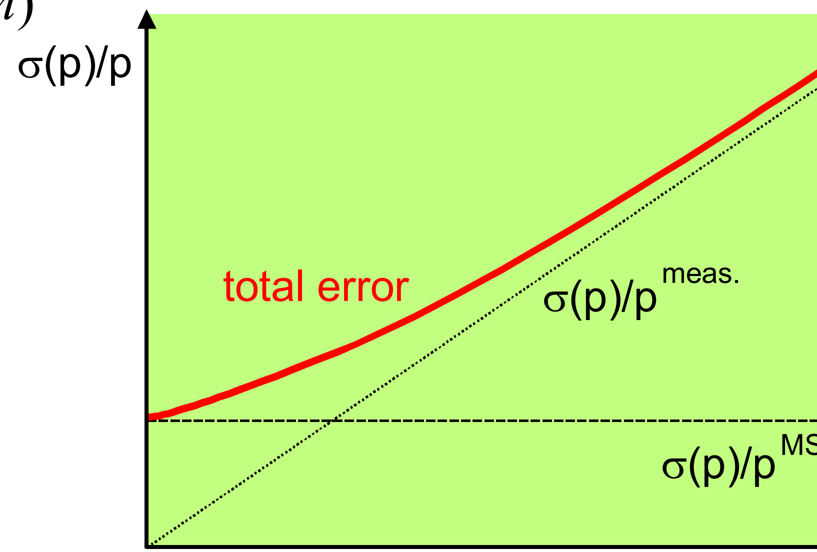

nergy loss by ionization: Bethe-Bloch

$$\left\langle \frac{dE}{dx}\right\rangle = -4\pi N_A r_e^2 m_e c^2 z^2 \frac{Z}{A}\frac{1}{\beta^2}\left[\frac{1}{2}\ln\frac{2m_e c^2\gamma^2\beta^2}{I^2}T^{max} - \beta^2 - \frac{\delta}{2}\right]$$

lE/dx in [MeV g^{-1} cm^2]

Bethe-Bloch formula only valid for “heavy” particles ($m \geq m_\mu$).

E/dx depends only on β,
dependent of m !

rst approximation:
edium simply
haracterized by

$\frac{Z}{A}$ **~ electron density**

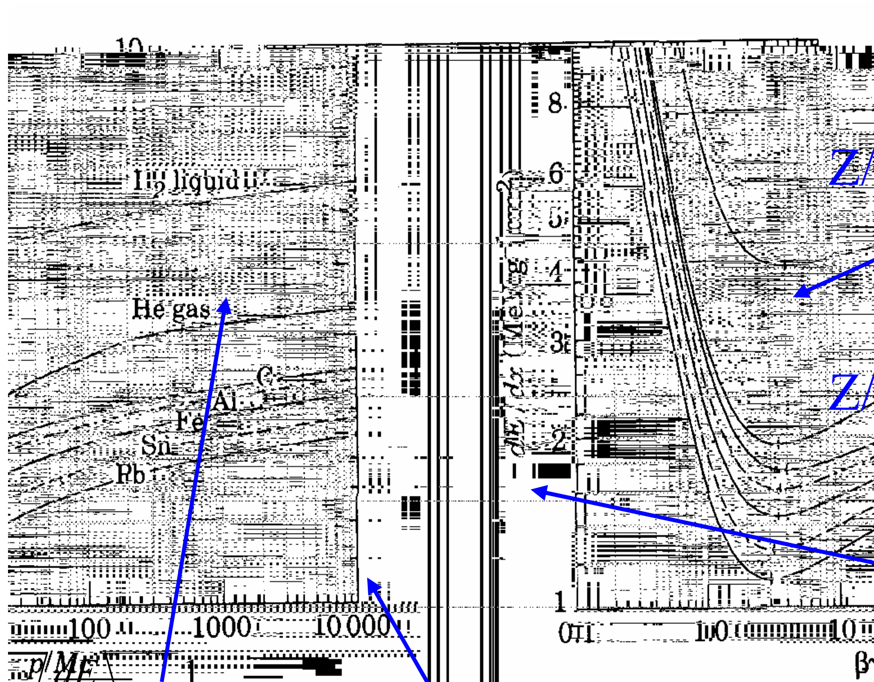

Landau tails

For thin layers (and low density materials):

→Few collisions, some with high energy transfer.

→ Energy loss distributions show large fluctuations towards high losses: "Landau tails"

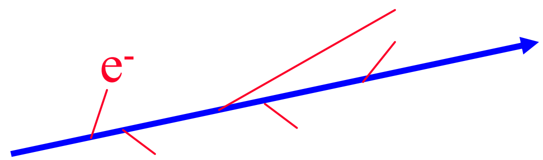

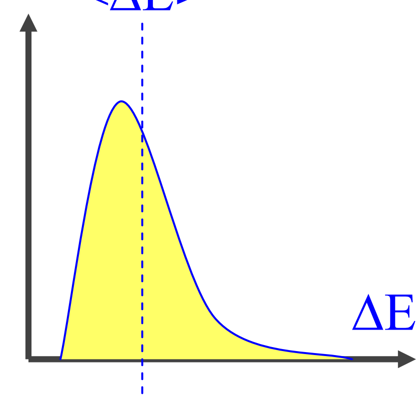

For thick layers and high density materials:

→ Many collisions.

→ Central Limit Theorem → Gaussian shape distributions.

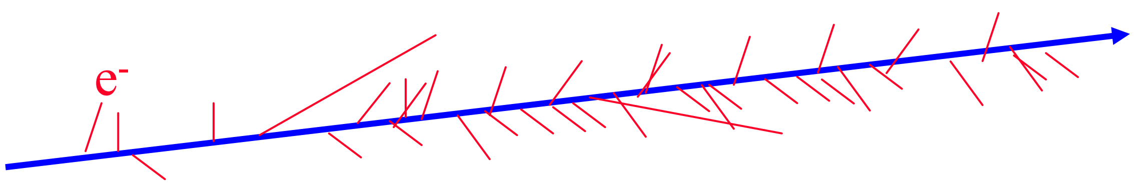

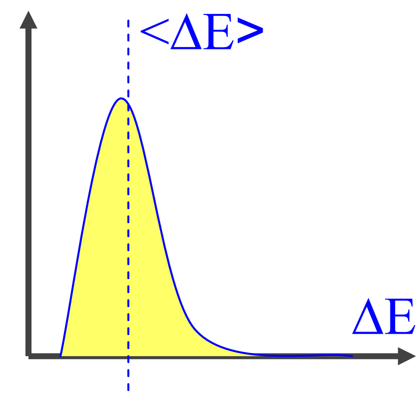

Ionization in Gas

ften the resulting primary electron will have enough kinetic energy to
nize other atoms.

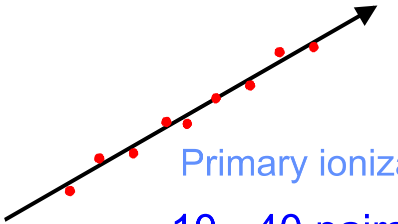

Primary ionization

10 - 40 pairs/cm
ΔE/pair ~ 20 - 40 eV

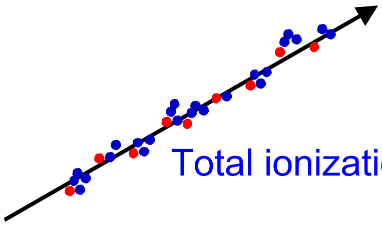

Total ionization

$$n_{total} \approx 3 \ldots 4 \cdot n_{primary}$$

Assume detector, 1 cm thick, filled with Ar gas:

1 cm

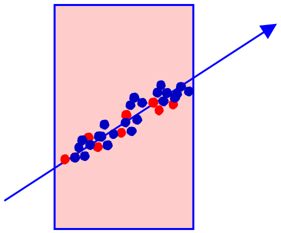

~ 100 e-ion pair

00 electron-ion pairs are not easy to detect!

oise of amplifier ≈1000 e- (ENC) !
e need to increase the number of e-ion pairs.

Amplification in gas

ectrons drift towards the anode wire

ose to the anode wire the field is sufficiently gh (some kV/cm), so that e^- gain enough ergy for further ionization → exponential crease of number of e^--ion pairs.

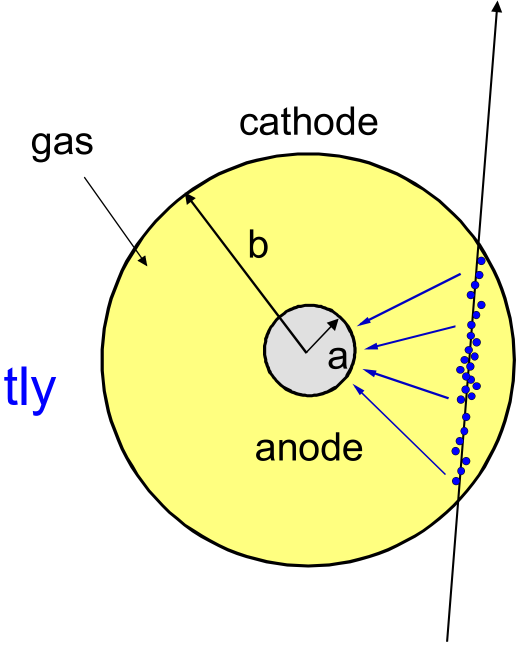

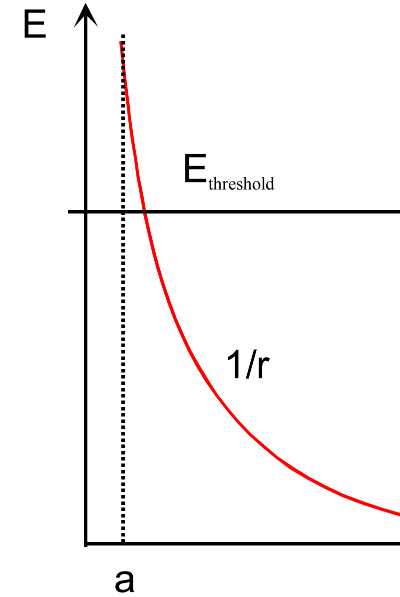

$$E(r) = \frac{CV_0}{2\pi\varepsilon_0} \cdot \frac{1}{r}$$

$$V(r) = \frac{CV_0}{2\pi\varepsilon_0} \cdot \ln \frac{r}{a}$$

Avalanche formation within a few wire radii and within t < 1 ns!

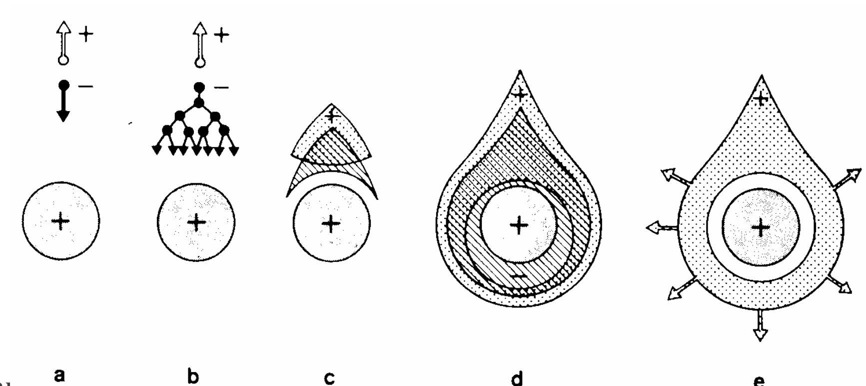

Signal formation

gnal induction both on anode and cathode due to moving
arges (both electrons and ions).

$$dv = \frac{Q}{lCV_0}\frac{dV}{dr}dr$$

ectrons collected by anode wire, i.e. *dr* is
nall (few μm). Electrons contribute only
ry little to detected signal (few %).

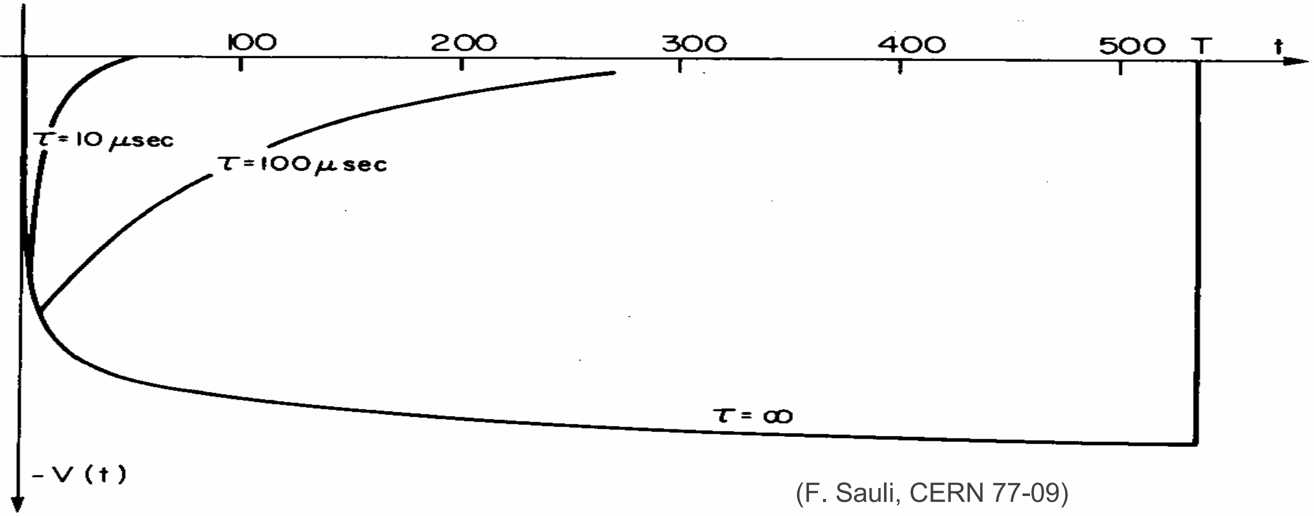

(F. Sauli, CERN 77-09)

Ions have to dri
back to cathode
i.e. *dr* is big.
Signal duration
limited by total
ion drift time !

Need electronic signal differentiation to limit dead time.

Multi wire proportional chambers

(G. Charpak et al. 1968, Nobel prize 1992)

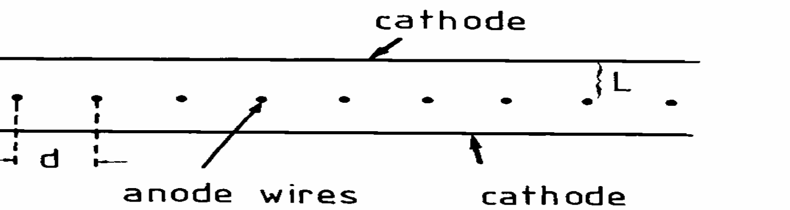

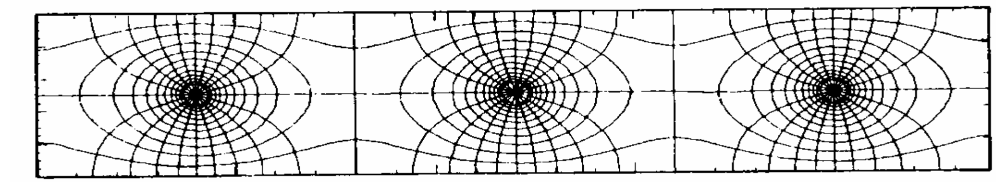

field lines and equipotentials around anode wires

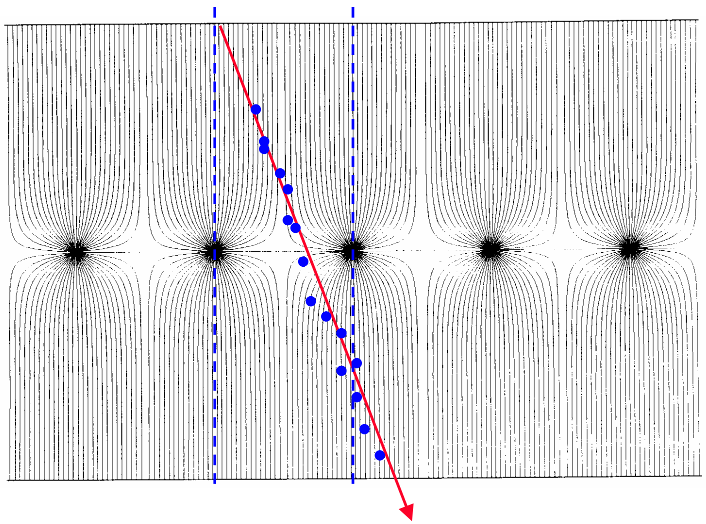

Typical parameters:

L=5mm, d=1mm,

a_{wire}=20mm.

Normally digital readout:
spatial resolution limited to

$$\sigma_x \approx \frac{d}{\sqrt{12}}$$

(d=1mm,
σ_x=300 μm)

Multi wire proportional chambers

Measuring the coordinate by induction

Example: 1 wire plane

+ 2 segmented

cathode planes

Analog readout of cathode planes.
→ $\sigma \approx 100\ \mu m$

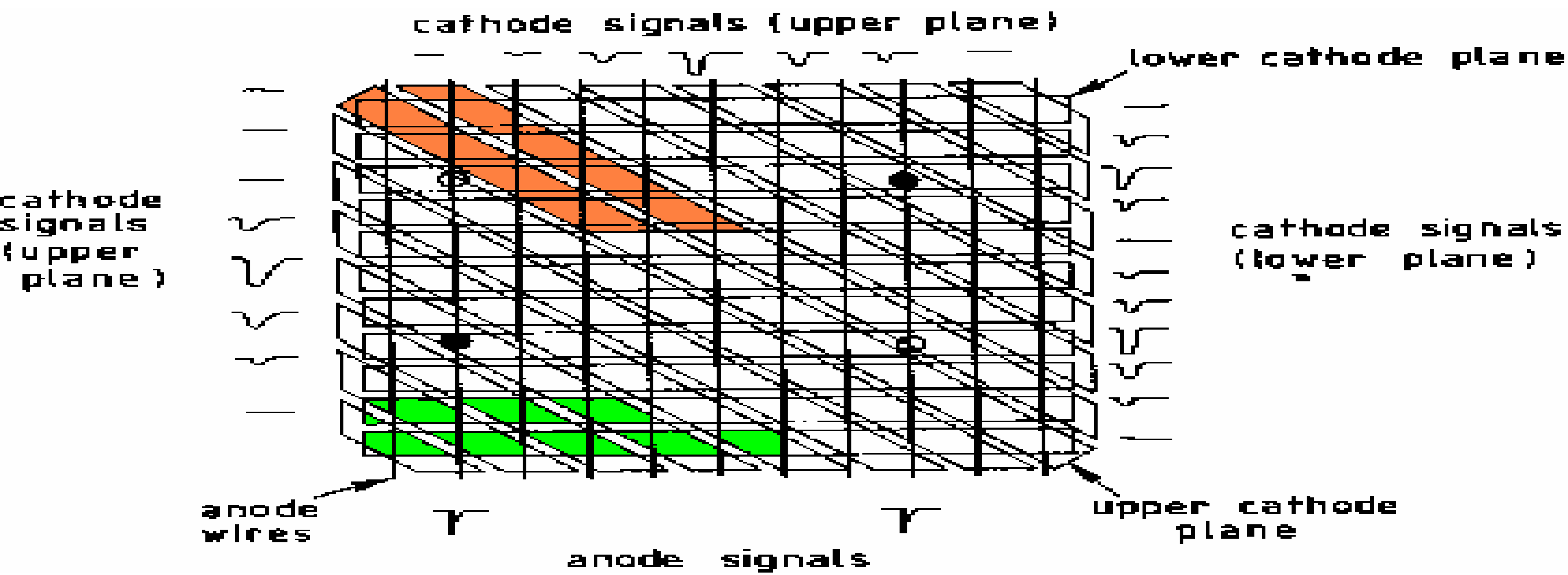

Resistive plate chambers (RPC)

No wires !

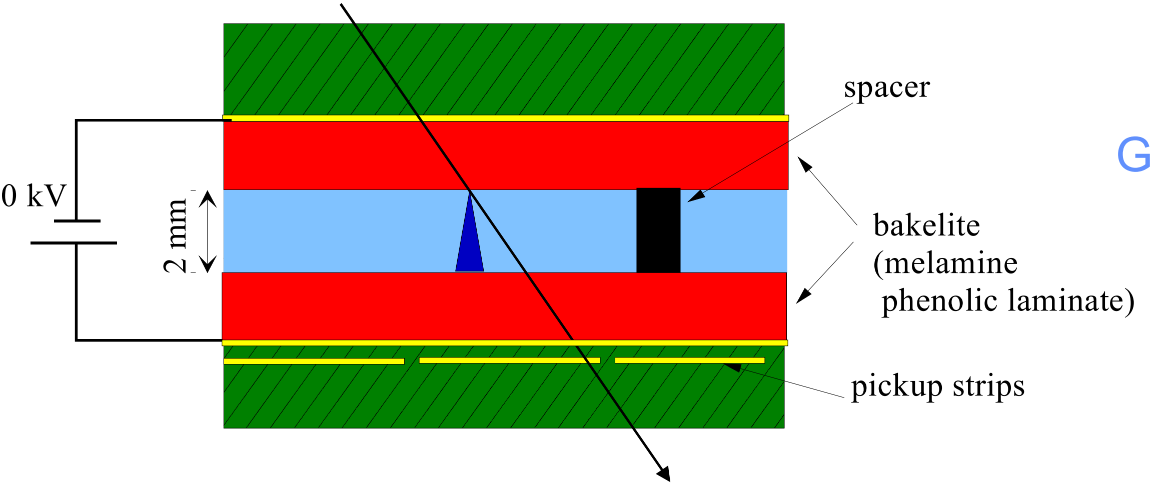

Gas: $C_2F_4H_2$, (C_2F_5H) + few % isobuta

Time dispersion ≈ 1..2 ns → suited as trigger chamber

Rate capability ≈ 1 kHz / cm^2

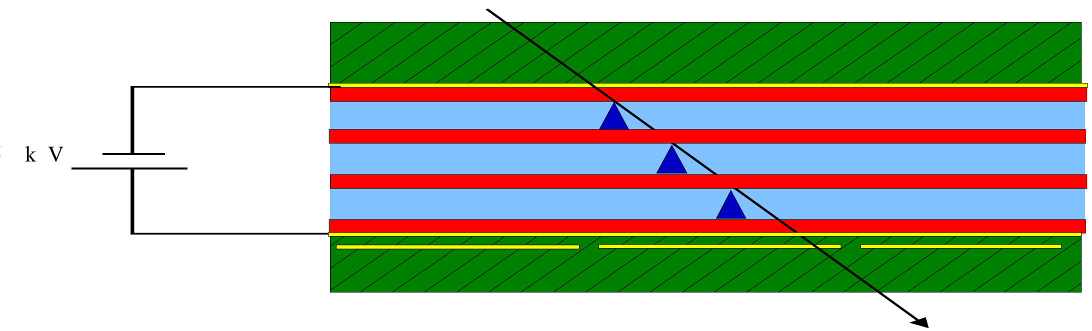

Double and multigap geometries → improve timing and efficiency

Problem: Operation close to streamer mode.

Drift chambers

First studies: T. Bressani, G. Charpak, D. Rahm, C. Zupancic, 1969
First operation drift chamber: A.H. Walenta, J. Heintze, B. Schürlein, NIM 92 (1971) 373)

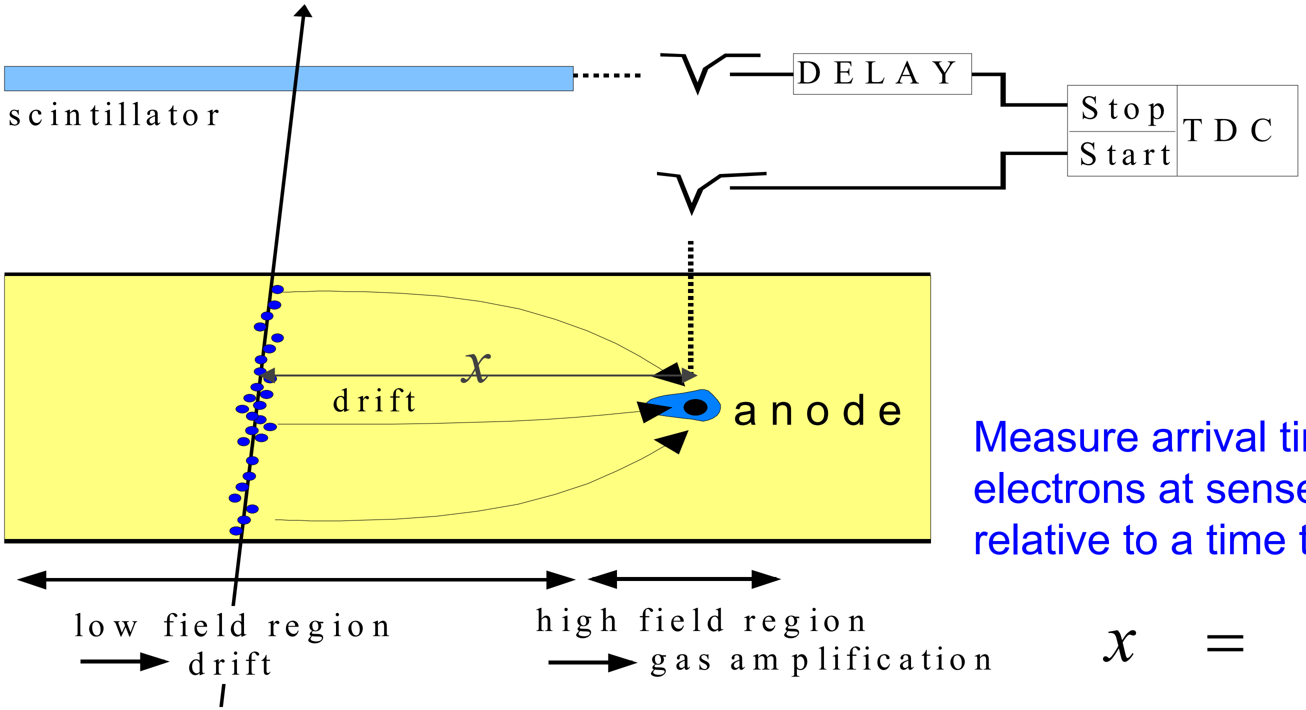

Measure arrival time of electrons at sense wire relative to a time t_0.

$$x = \int v_D(t)\, dt$$

What happens during the drift towards the anode wire ?

- ☞ Diffusion ?
- ☞ Drift velocity ?

Drift and diffusion in gases

No external fields:

ectrons and ions will lose their energy due to collisions with the gas atoms → ermalization

$$\varepsilon = \frac{3}{2} kT \approx 40 \quad \text{meV}$$

dergoing multiple collisions, an originally localized ensemble of charges will diffuse

$$\frac{dN}{N} = \frac{1}{\sqrt{4\pi Dt}} e^{-(x^2/4Dt)} dx$$

$$\sigma_x(t) = \sqrt{2Dt} \quad or \quad D = \frac{\sigma_x^2(t)}{2t}$$

D: diffusion coefficient

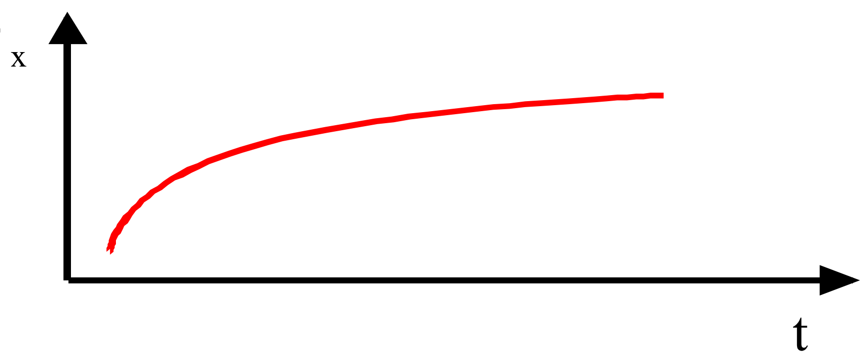

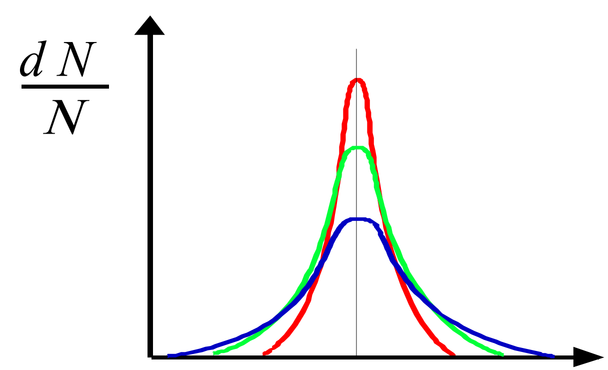

Drift and diffusion in gases

External electric field

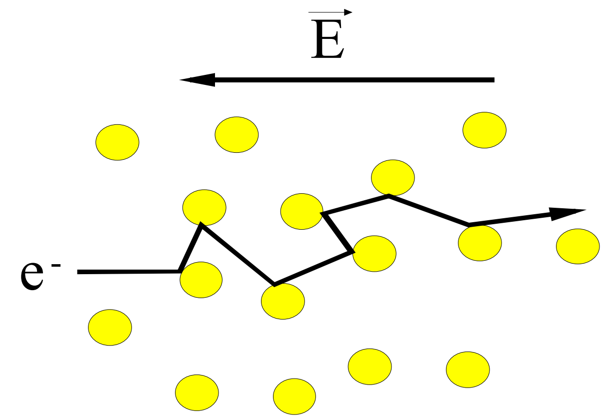

top and go" traffic due to scattering
om gas atoms $\rightarrow$ drift

$$\vec{v}_D = \mu \vec{E}$$

$$\mu = \frac{e\tau}{m} \quad \text{(mobility)}$$

the equilibrium ...

λ_ε : fractional energy loss / collision

$$\frac{x}{v_D \tau} \lambda_\varepsilon \varepsilon = eEx$$

$$\tau = \frac{1}{N\sigma v}$$

v: instantaneous velocity

Time needed to move by x

Drift and diffusion in gases

in the equilibrium ...

$$\frac{x}{v_D \tau} \lambda_\varepsilon \varepsilon = eEx$$

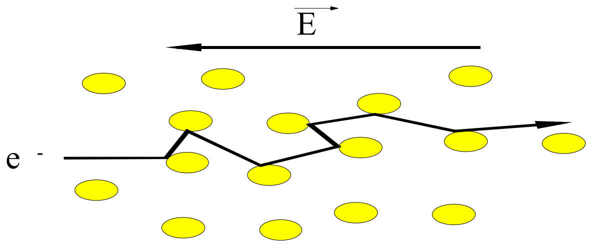

λ_ε : fractional energy loss / collision

$\tau = \frac{1}{N \sigma v}$ v: instantaneous velocity

$$\Rightarrow \quad v_D^2 = \frac{eE}{mN\sigma}\sqrt{\frac{\lambda}{2}}$$

$\sigma = \sigma(\varepsilon)$!

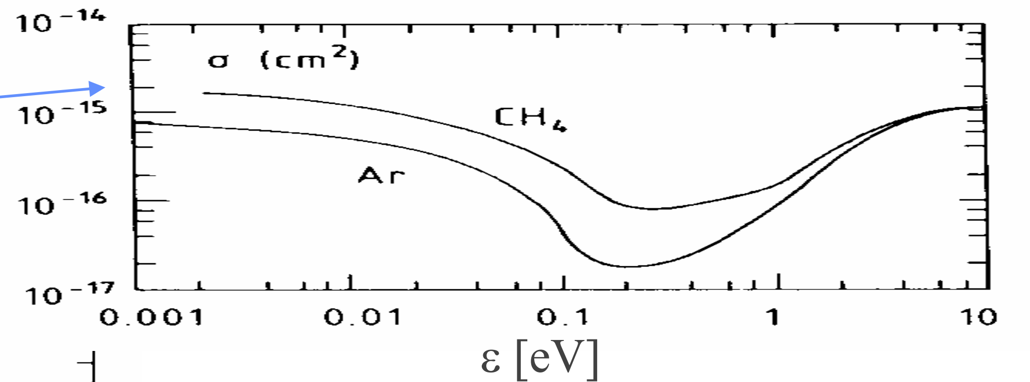

(B. Schmidt, thesis, unpublished, 1986)

$\lambda = \lambda(\varepsilon)$!

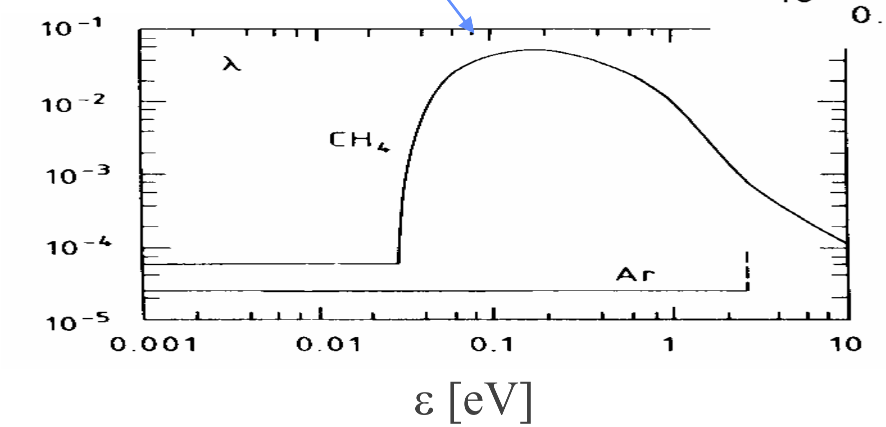

Typical electron drift velocity: **5 cm/μs** Ion drift velocities: ca. 1000 times smaller

Drift and diffusion in gases

In the presence of electric and magnetic fields, drift and diffusion are driven by $\vec{E} \times \vec{B}$ **effects**

Look at 2 special cases:

Special case: $\vec{E} \perp \vec{B}$

$$\tan \alpha_L = \omega\tau$$

α_L: Lorentz angle

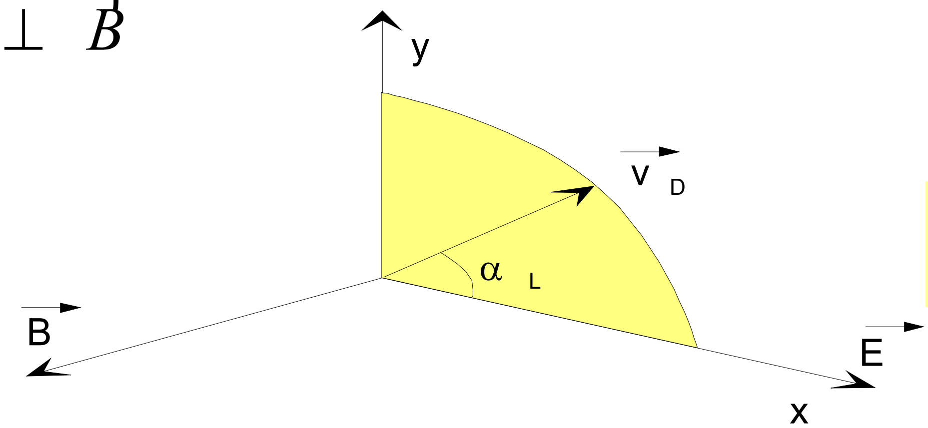

$$\vec{v}_D \nparallel \vec{E}$$

$$\omega = \frac{e\vec{B}}{m}$$

cyclotron frequency

Drift and diffusion in gases

Special case: $\vec{E} \parallel \vec{B}$

The longitudinal diffusion (along B-field) is unchanged.
In the transverse projection the electrons are forced on circle segments with the radius v_T/ω.
The transverse diffusion coefficient appears reduced

$$D_T(B) \approx \frac{D_0}{1+\omega^2\tau^2}$$

Very useful… see later !

Transverse diffusion σ (μm) for a drift of 15 cm in different Ar/CH_4 mixtures

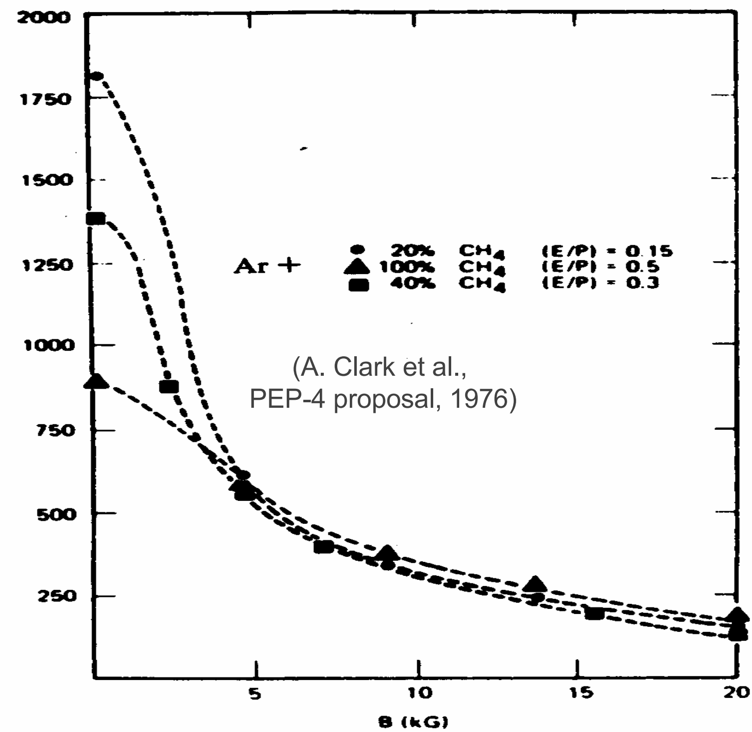

Drift chambers

Some planar drift chamber designs

Optimize geometry → constant E-field
Choose drift gases with little dependence $v_D(E)$
→ linear space - time relation r(t)

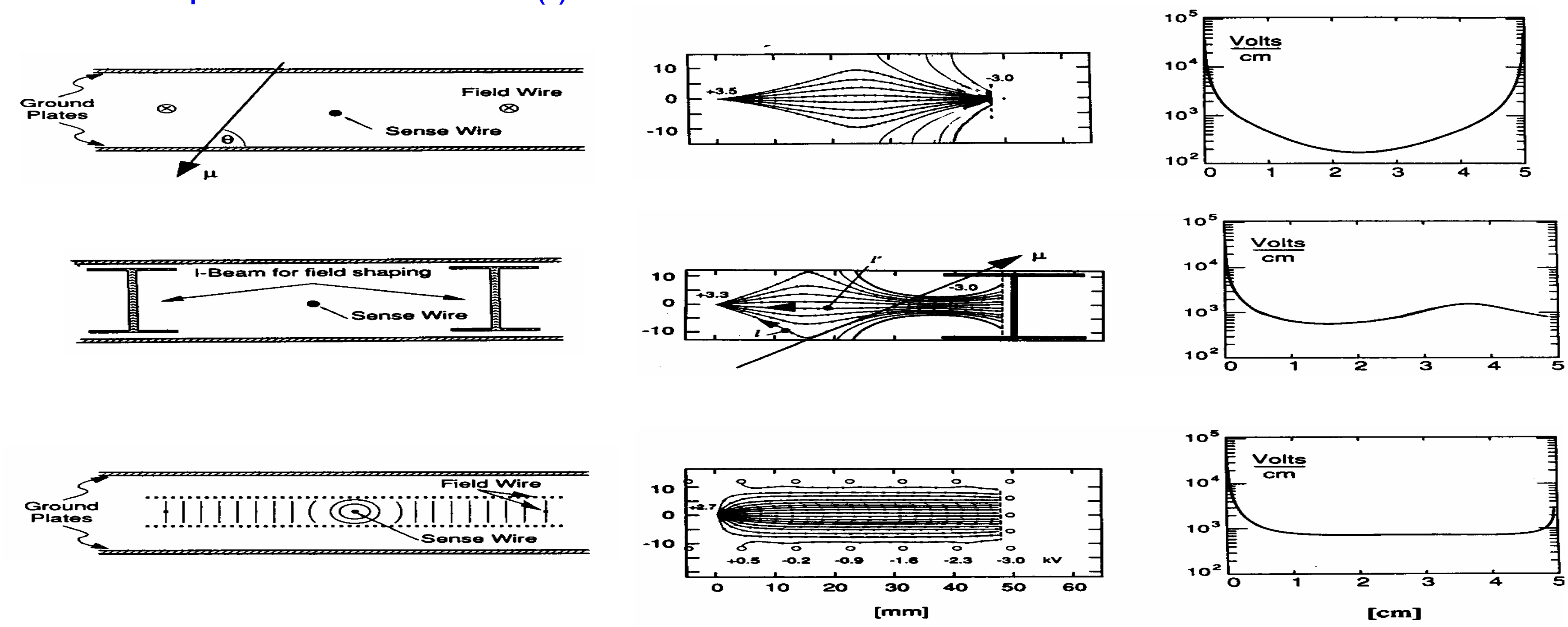

(U. Becker, in: Instrumentation in High Energy Physics, World Scientific)

The spatial resolution is not limited by the cell size
→ less wires, less electronics,
less support structure than in MWPC.

Drift chambers

Resolution determined by
- diffusion,
- path fluctuations,
- electronics
- primary ionization statistics

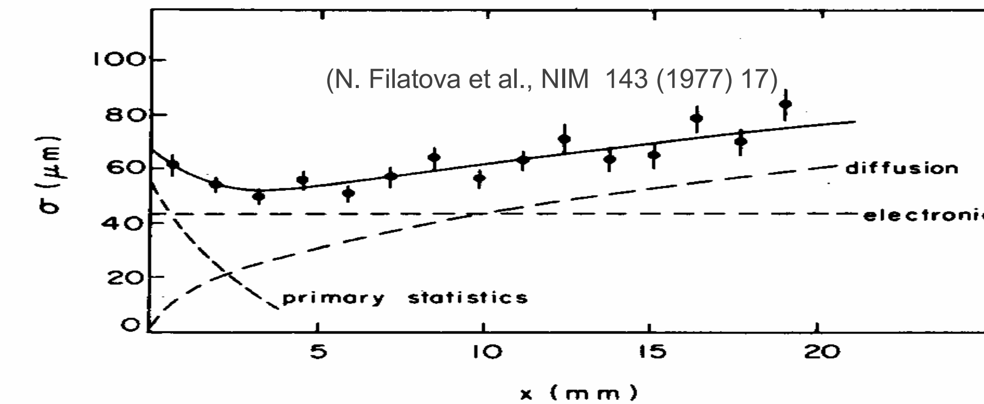

Various geometries of cylindrical drift chambers

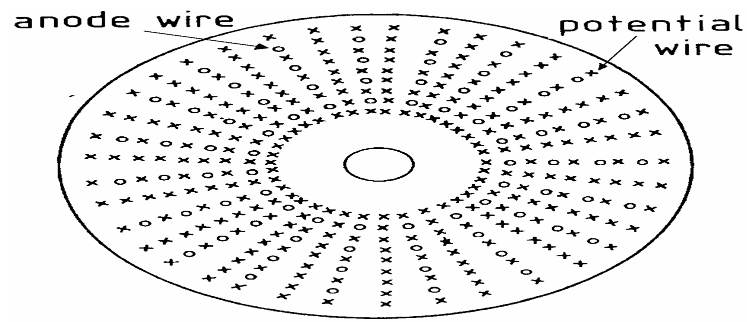

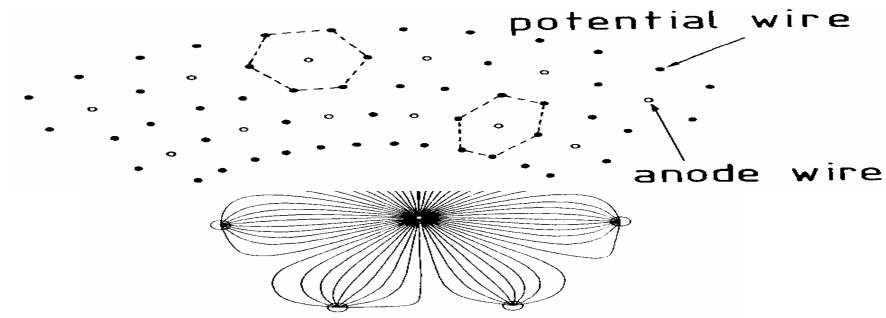

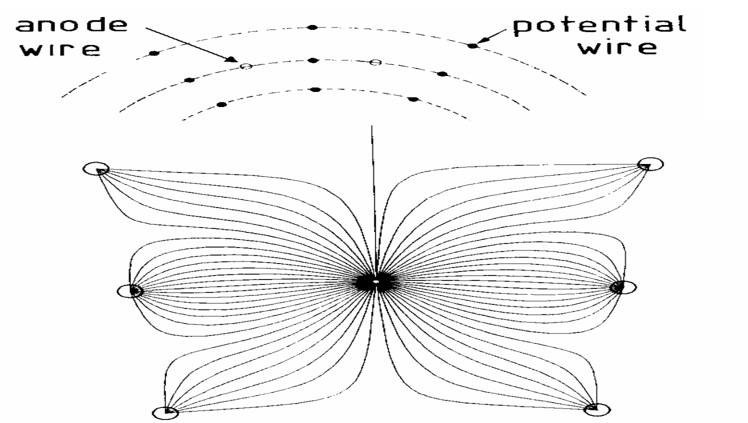

Drift Chambers

Time Projection Chamber → full 3-D track reconstruction

x-y from wires and segmented cathode of MWPC

z from drift time

in addition dE/dx information

Diffusion significantly reduced by B-field.

PEP-4 TPC

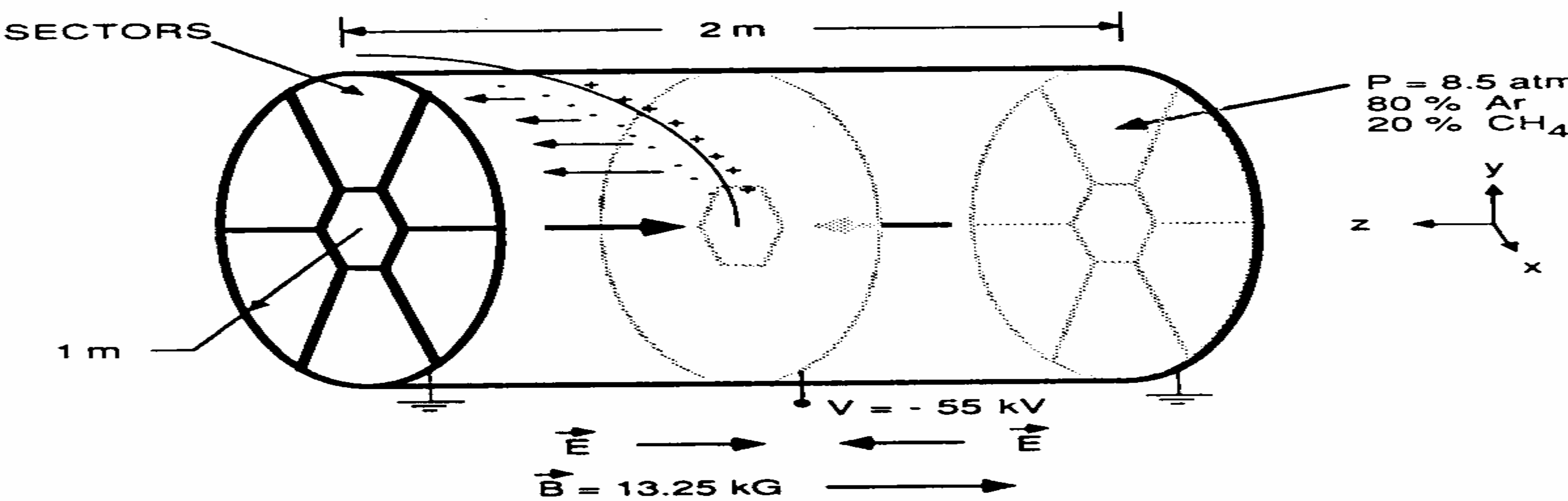

Drift Chambers

Drift over long distances → very good gas quality required

Requires precise knowledge of v_D → LASER calibration + p,T corrections

Space charge problem from positive ions, drifting back to midwall → gating

ALEPH TPC

ALEPH coll., NIM A 294 (1990) 121,
Atwood et. Al, NIM A 306 (1991) 446)

Ø 3.6M, L=4.4 m

$\sigma_{R\phi} = 173\ \mu m$
$\sigma_z = 740\ \mu m$
(isolated leptons)

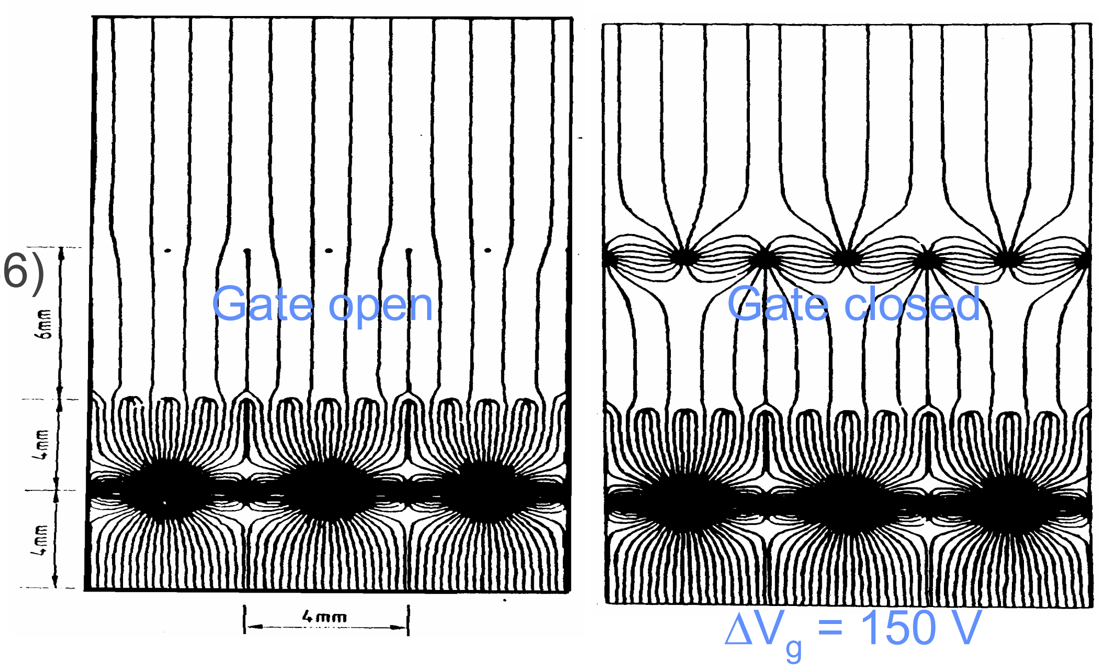

Micro gaseous detectors

Faster and more precision ? → smaller structures

(A. Oed, NIM A 263 (1988) 352)

Microstrip gas chamber

geometry and typical dimensions
(former CMS standard)

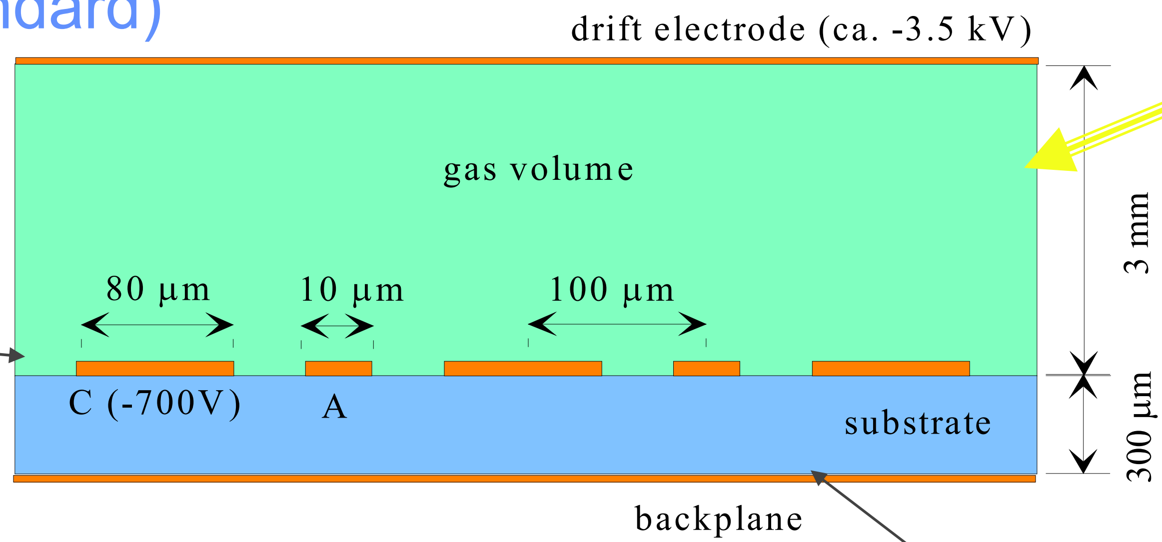

Only 30 ion-electron pairs

Gold strips
+ Cr under layer

Glass DESAG AF45 + S8900
semiconducting glass coating, $\rho=10^{16}$ $\Omega/\Box$

Micro gaseous detectors

Field geometry

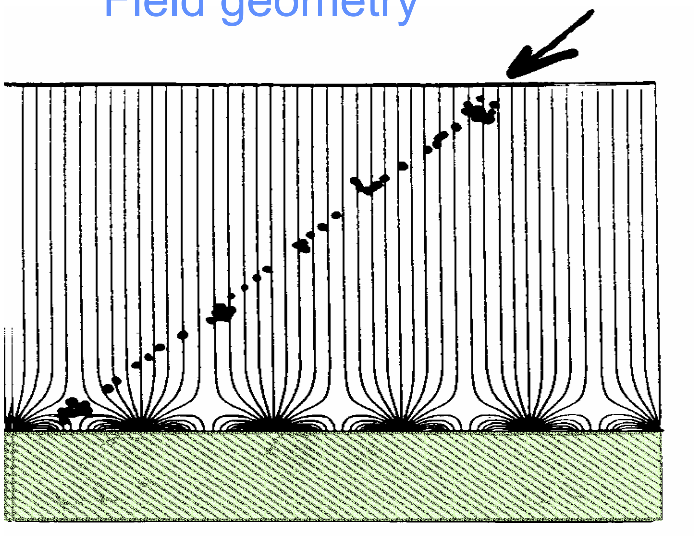

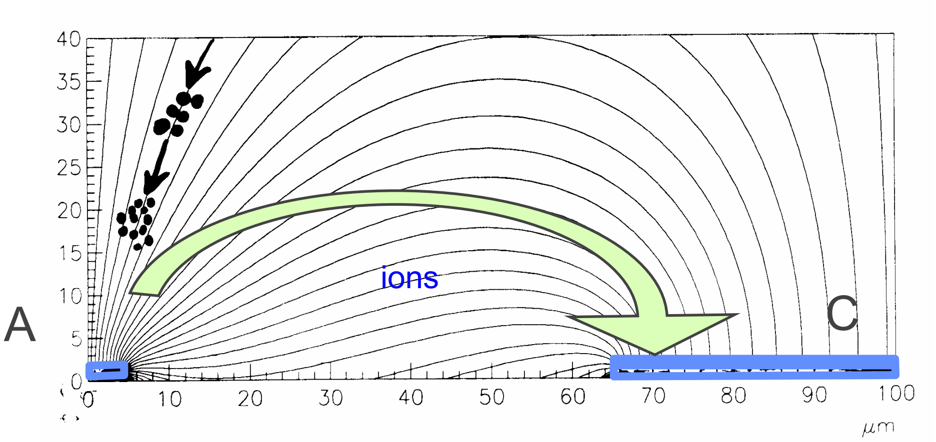

Fast ion evacuation → high rate capability
≈ 10^6 /(mm^2·s)

Gas: Ar-DME, Ne-DME (1:2), Lorentz angle 14º at 4T.

Gain ≤10^4

Passivation: non-conductive protection of cathode edges

Resolution: ≈ 30..40 µm

Aging: Seems to be under control.

10 years LHC operation ≈ 100 mC/cm

Micro gaseous detectors

- GEM: The Gas Electron Multiplier

(R. Bouclier et al., NIM A 396 (1997) 50)

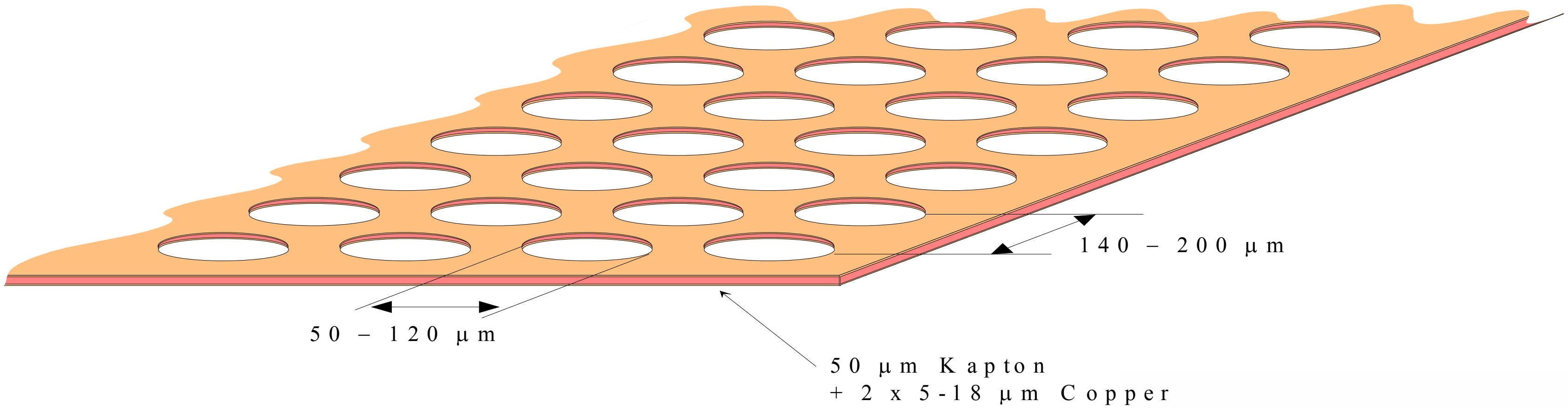

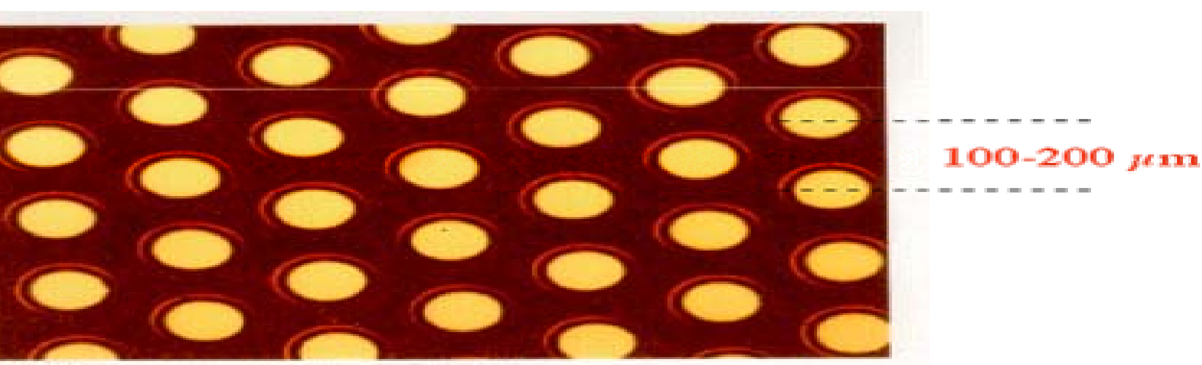

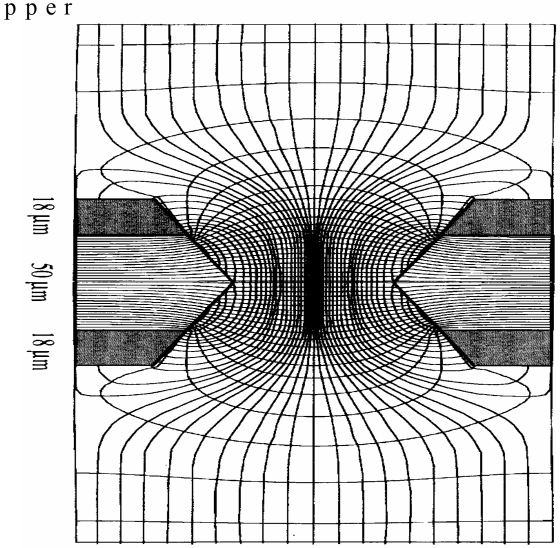

Micro photo of a GEM foil

Micro gaseous detectors

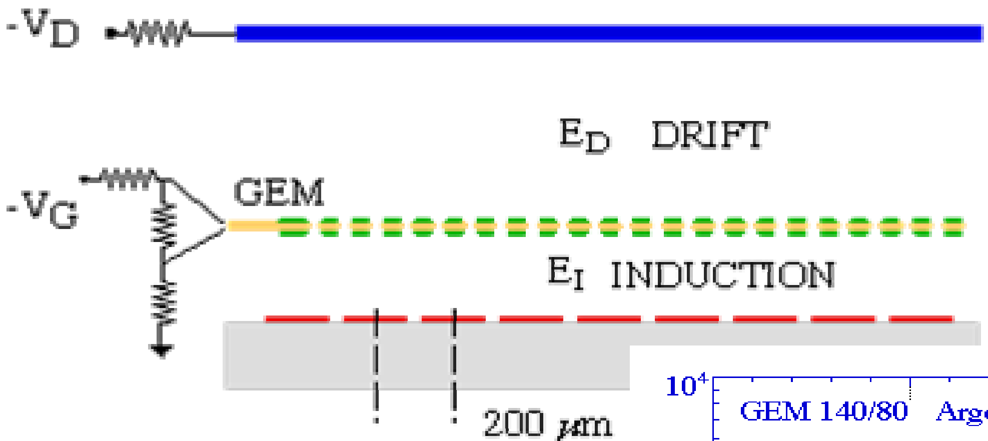

Single GEM

+ readout pads

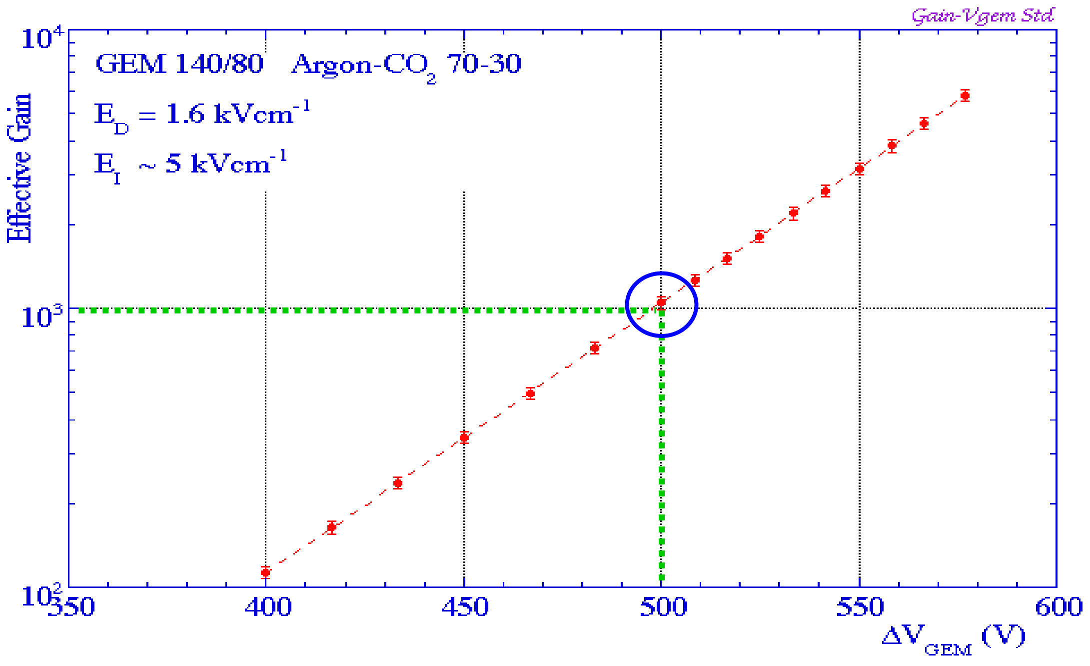

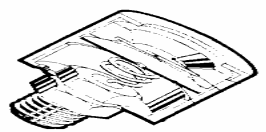

Silicon detectors

Solid state detectors have a long tradition for energy measurements (Si, Ge, Ge(Li)).

Here we are interested in their use as precision trackers !

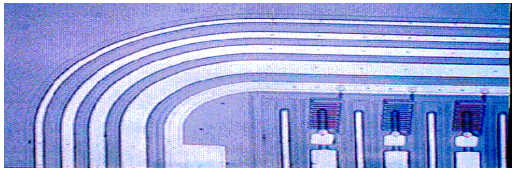

Silicon detectors

Some characteristic numbers for silicon

- Band gap: E_g =1.12 V.
- E(e^--hole pair) = 3.6 eV, (≈ 30 eV for gas detectors).
- High specific density (2.33 g/cm^3) → ΔE/track length for M.I.P.'s.: 390 eV/μm ≈ 108 e-h/ μm (average)
- High mobility: μ_e =1450 cm^2/Vs, μ_h = 450 cm^2/Vs
- Detector production by microelectronic techniques → small dimensions → fast charge collection (<10 ns).
- Rigidity of silicon allows thin self supporting structures. Typical thickness 300 μm → ≈ $3.2 \cdot 10^4$ e-h (average)
- But: No charge multiplication mechanism!

Silicon detectors

How to obtain a signal ?

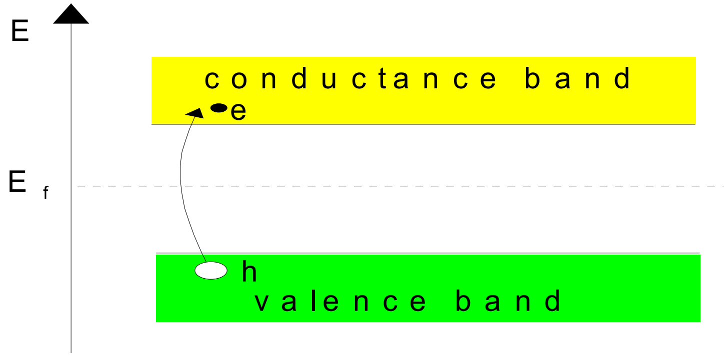

For Silicon: $n_i \approx 1.45 \cdot 10^{10}$ cm^{-3}

In a pure intrinsic (undoped) material the electron density n and hole density p are equal. $n = p = n_i$

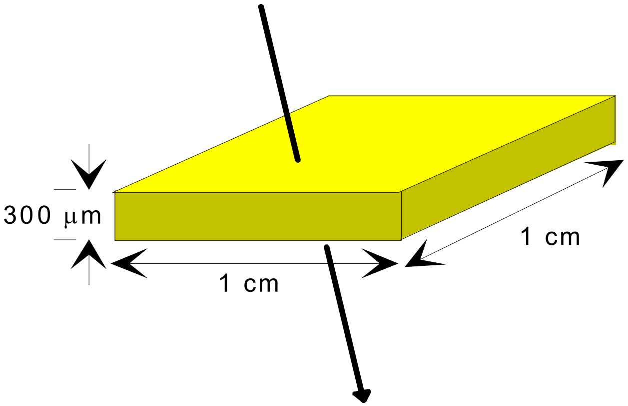

In this volume we have $4.5 \cdot 10^8$ free charge carriers, but only $3.2 \cdot 10^4$ e-h pairs produced by a M.I.P.

→ Reduce number of free charge carriers, i.e. deplete the detector

Most detectors make use of reverse biased p-n junctions

Silicon detectors

Doping

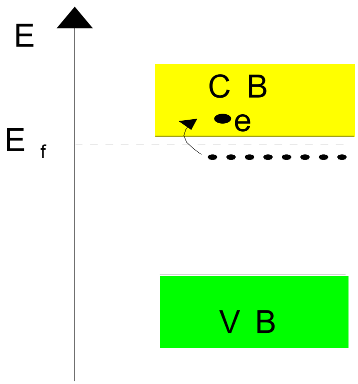

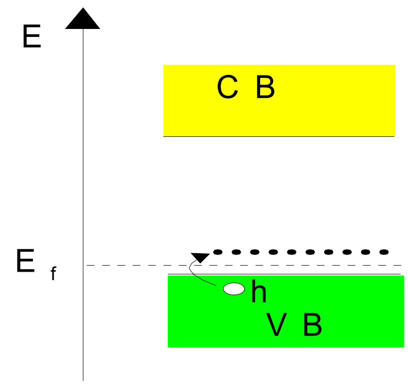

n-type: Add elements from Vth group, donors, e.g. As.
Electrons are the majority carriers.

p-type: Add elements from IIIrd group, acceptors, e.g. B.
Holes are the majority carriers.

	detector grade	electronics grade
doping concentration	10^{12} cm^{-3} (n) - 10^{15} cm^{-3} (p^{+})	$10^{17(18)}$ cm^{-3}
resistivity	≈ 5 kΩ·cm	≈1 Ω·cm

silicon detectors pn junction

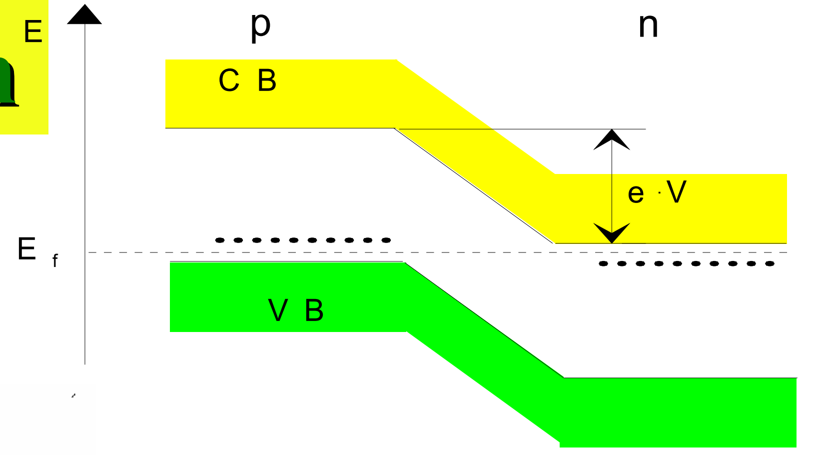

There must be a single Fermi level !
Deformation of band structure →
potential difference.

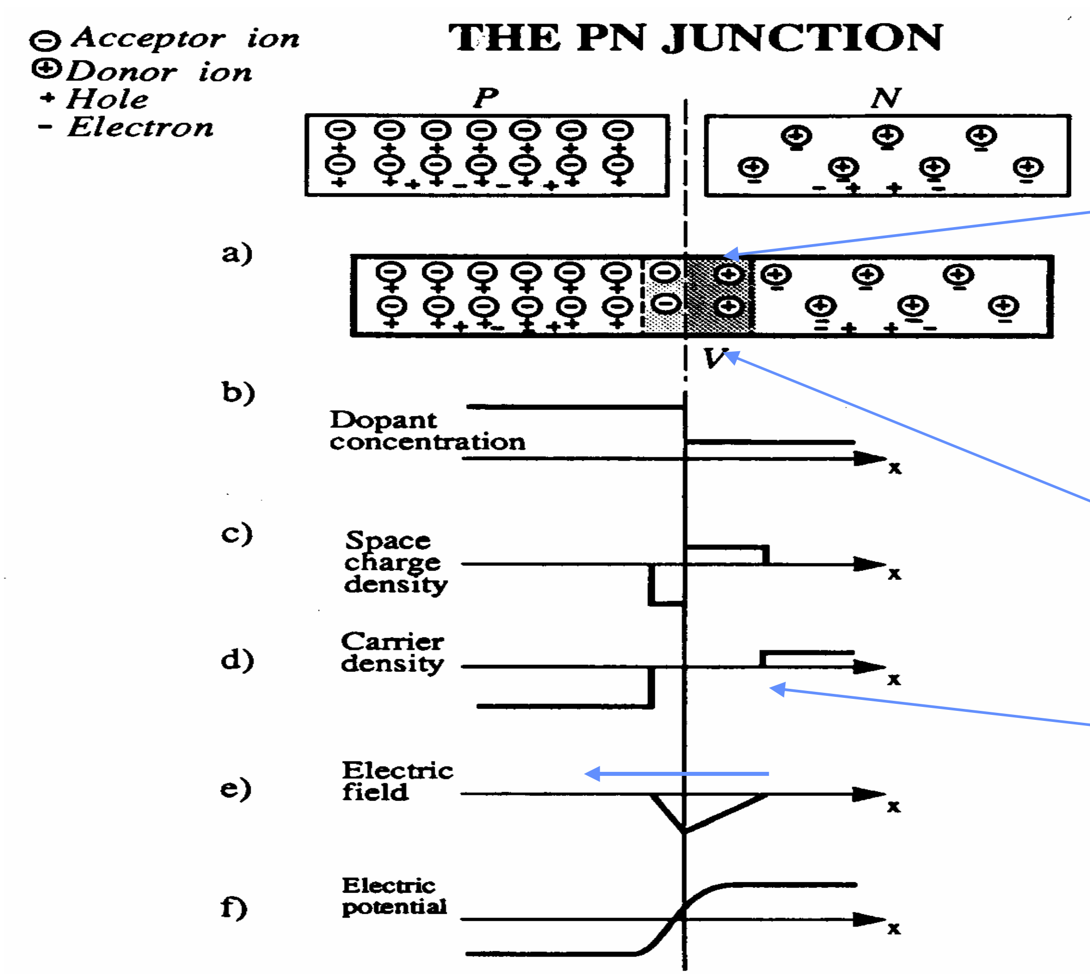

diffusion of e⁻ into p-zone, h⁺ into n-zone
→ potential difference stopping diffusion

thin depletion zone

no free charge carriers
in depletion zone

(A. Peisert, Instrumentation In High Energy Physics, World Scientific)

Silicon detectors

Spatial information by segmenting the p doped layer →

- Application of a reverse bias voltage (about 100V) → the thin depletion zone gets extended over the full junction → fully depleted detector.
- Energy deposition in the depleted zone, due to traversing charged particles or photons (X-rays), creates free e⁻-hole pairs.
- Under the influence of the E-field, the electrons drift towards the n-side, the holes towards the p-side → detectable current.

(A. Peisert, Instrumentatio
In High Energy Physics,
World Scientific)

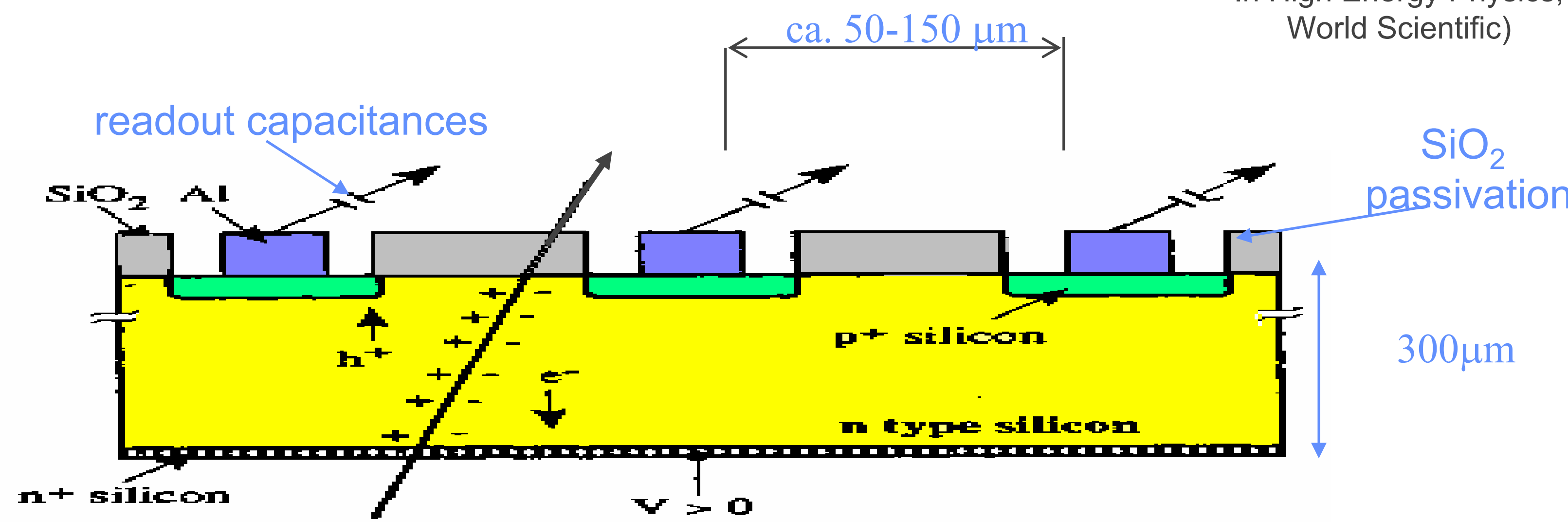

defines end of depletion zone
+ good ohmic contact

Silicon detectors

Silicon pixel detectors

- Segment silicon to diode matrix
- also readout electronic with same geometry
- connection by bump bonding technique

Flip-chip technique

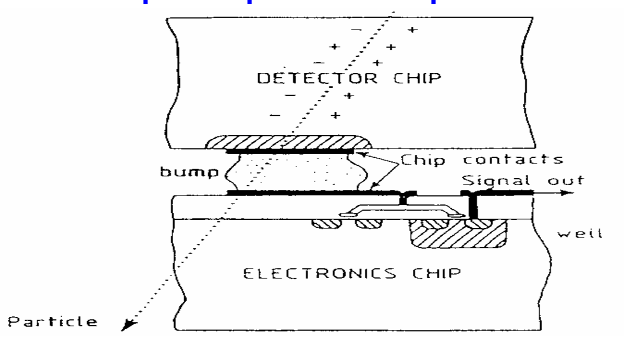

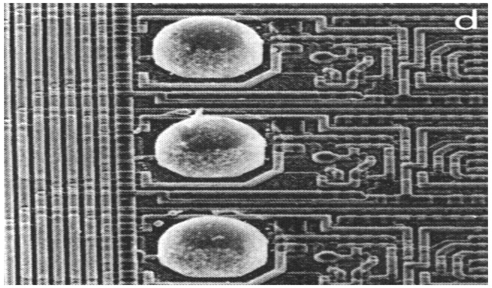

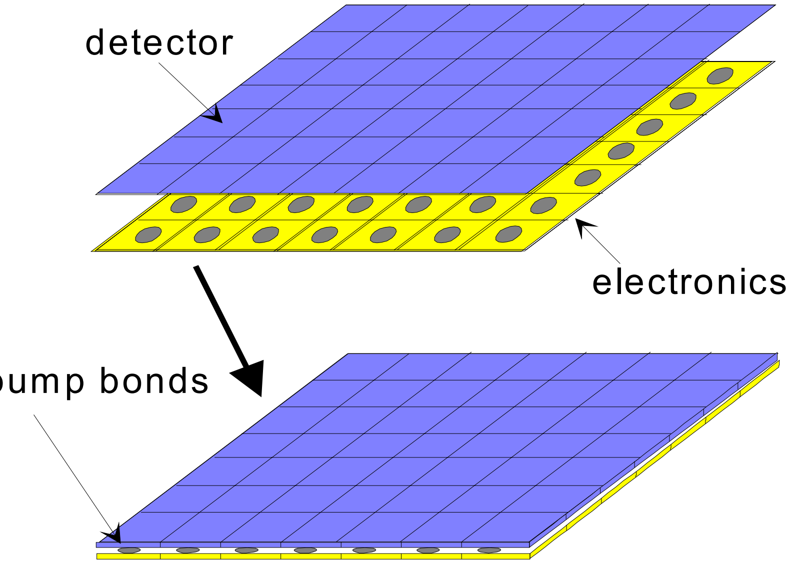

RD 19, E. Heijne et al., NIM A 384 (1994) 399

Requires sophisticated readout architecture
First experiment WA94 (1991), WA97
OMEGA 3 / LHC1 chip (2048 pixels, 50x500 mm2) (CERN ECP/96-03)
Pixel detectors will be used also in LHC experiments (ATLAS, ALICE, CMS)

Silicon Detectors

The DELPHI micro vertex detector (since 1996)

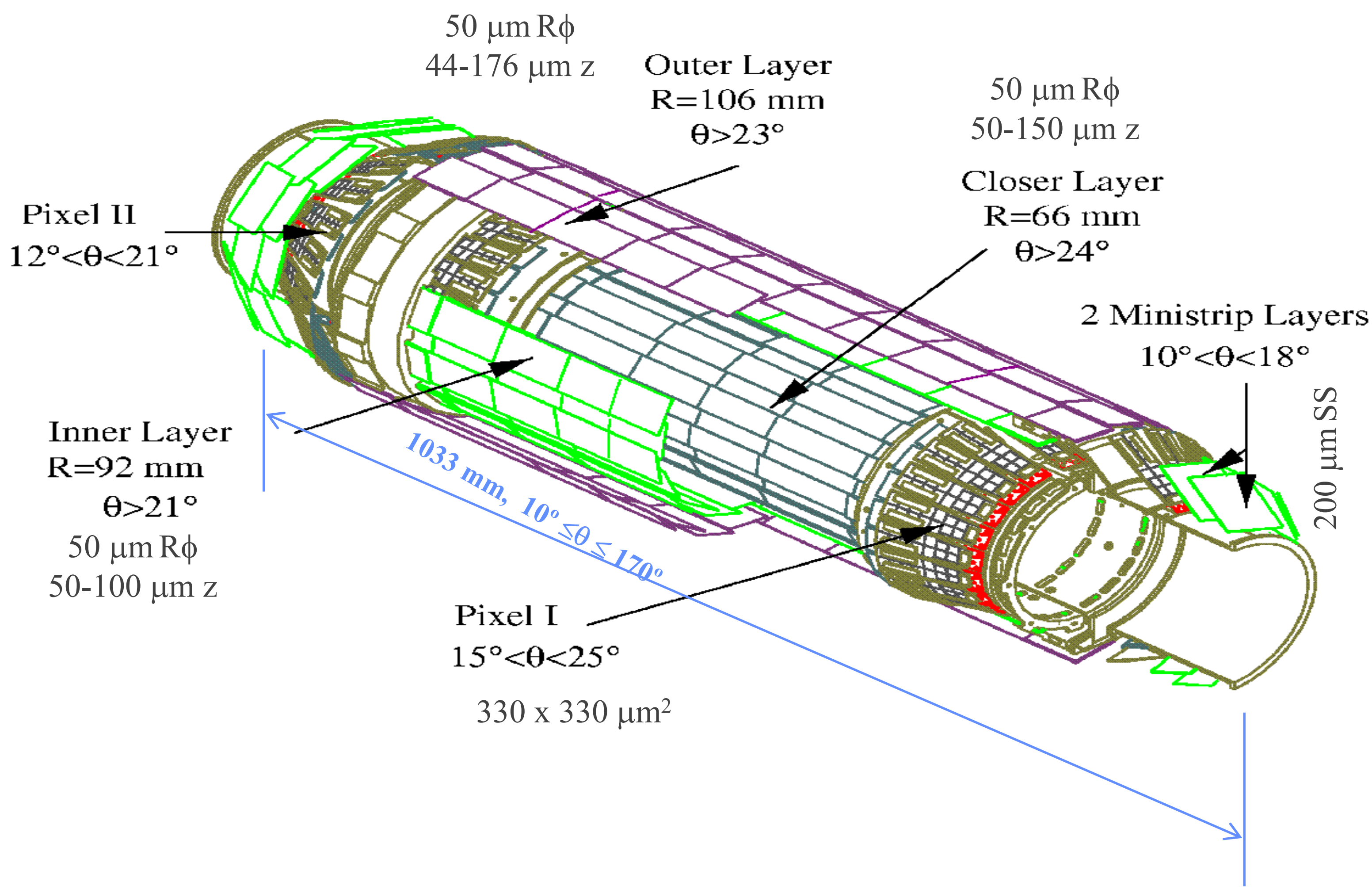

Silicon Detectors

Delphi

adout channels:
. 174 k strips, 1.2 M pixels
tal readout time: 1.6 ms
otal dissipated power 400 W →
ater cooling system
t resolution in barrel part ≈ 10 μm
pact parameter resolution (rϕ)

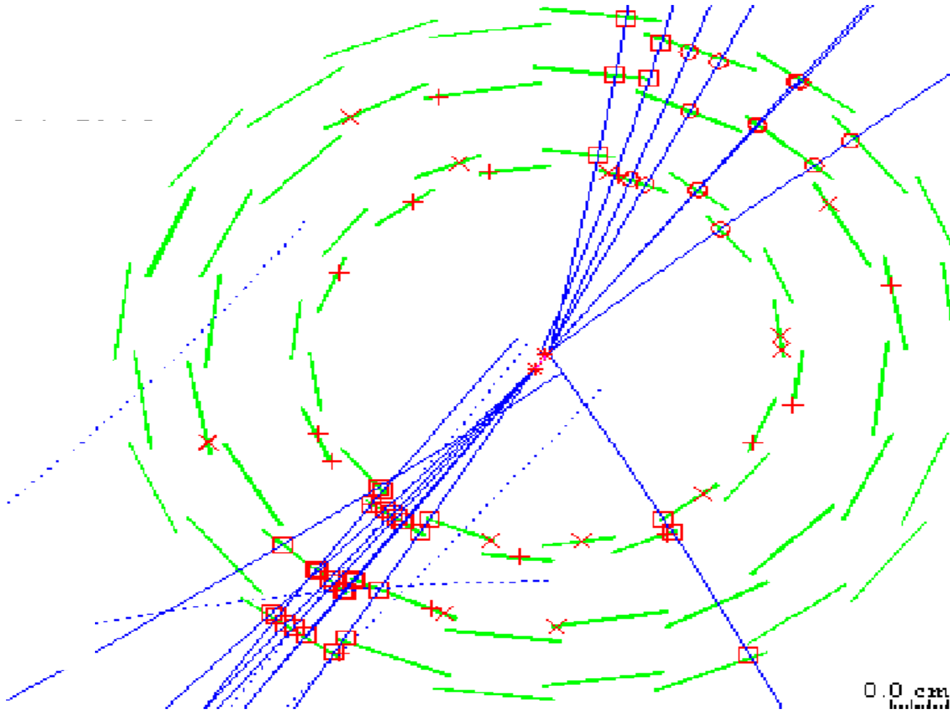

$$28 \quad \mu m \quad \oplus \quad 71 \quad / \left(p \sin^{\frac{3}{2}} \theta \right)$$

SLD Microvertex

Vertex detectors CCD's, pixels):

- At SLC: inner radius **2.3 cm**, superior resolution.

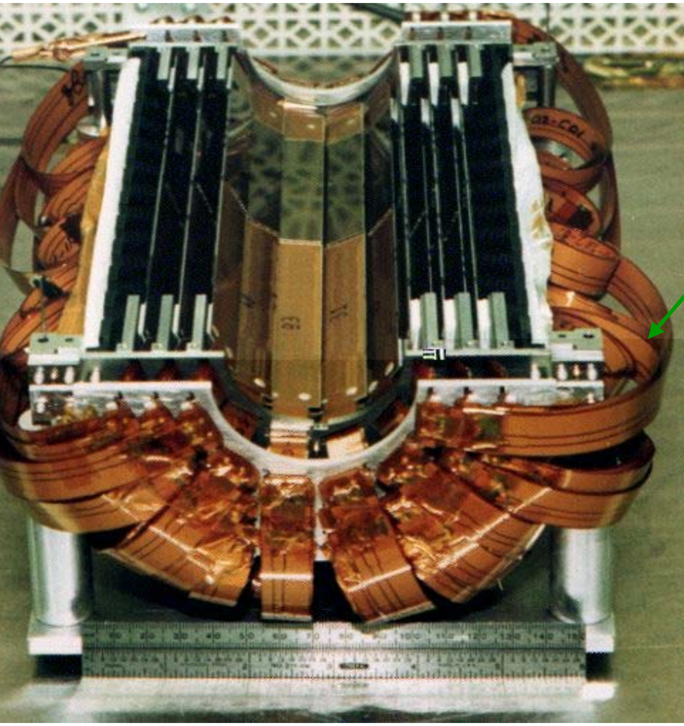

SLD can do both b- and c-tagging with good purity.